Determination of Phonon Dispersions from X-Ray Transmission Scattering: The Example of Silicon

M. Holt,[1,2] Z. Wu,[1,3] Hawoong Hong,[1] P. Zschack,[1] P. Jemian,[1] J. Tischler,[4] Haydn Chen,[1,3] and T.-C. Chiang[1,2,*]

[1]*Frederick Seitz Materials Research Laboratory, University of Illinois at Urbana-Champaign, 104 South Goodwin Avenue, Urbana, Illinois 61801-2902*

[2]*Department of Physics, University of Illinois at Urbana-Champaign, 1110 West Green Street, Urbana, Illinois 61801-3080*

[3]*Department of Materials Science and Engineering, University of Illinois at Urbana-Champaign, 1304 West Green Street, Urbana, Illinois 61801-2980*

[4]*Solid State Division, Oak Ridge National Laboratory, Oak Ridge, Tennessee 37831-6033*

(Received 6 May 1999)

A beam of monochromatic synchrotron x-ray incident on a silicon wafer creates a rich intensity pattern behind the wafer that reflects the cross section of scattering by thermally populated phonons. A least-squares fit of the patterns based on a lattice dynamics calculation yields the phonon dispersion relations over the entire reciprocal space. This simple and efficient method is suitable for phonon studies in essentially all materials, and complements the traditional neutron scattering technique.

PACS numbers: 78.70.Ck, 63.20.Dj

Phonons are the fundamental quanta of lattice vibration in a solid. They play a critical role in phenomena such as superconductivity and many types of phase transitions, and are the basis for the acoustic, thermal, elastic, and infrared properties of solids [1]. A fundamental description of phonons is the dispersion relation, which is determined traditionally through neutron scattering [2–4] or, more recently, through inelastic x-ray scattering [5]. However, these methods can be technically demanding, and alternative, complementary methods have been long sought. This study demonstrates a new approach based on x-ray intensity patterns produced by scattering from thermally populated phonons using silicon as a test case. Intensity patterns with a wide dynamic range were recorded in a matter of seconds at the third-generation synchrotron, the Advanced Photon Source. A least-squares analysis in terms of lattice dynamics yields dispersions for all six phonon branches in excellent agreement with neutron scattering results. The fast data acquisition rate, simplicity of the experiment, and a minimal requirement on sample volume make this method attractive for a wide range of applications in materials research.

Although intensity distribution of x-ray scattering by thermally populated phonons has been long recognized as a possible measure of phonon properties [6–8], this method has remained impractical and attracted little interest. The situation has changed due to recent advances in synchrotron radiation instrumentation and computational power. Undulator beams at third-generation synchrotrons, such as the Advanced Photon Source, now yield a brightness about 8 orders of magnitude higher than a conventional laboratory source. In addition, the use of two-dimensional detectors such as the image plate used in this experiment allows parallel detection over a large scattering solid angle, effectively increasing the data collection rate by 6 orders of magnitude. The combined improvement makes it possible to carry out such measurements with a high degree of precision and efficiency. Intensity patterns recorded from both Si(111) and Si(100) in a transmission mode, displayed on a logarithmic scale, reveal details of intensity variation that are uniquely related to phonon modes over a wide range in the reciprocal space, thus enabling a determination of the phonon dispersions.

Our experiment was performed at the undulator beam line of Sector 33 (University, Industry, and National Laboratory Collaborative Access Team) at the Advanced Photon Source. A transmission Laue geometry was employed, in which a 28 keV beam was sent at normal incidence through commercial Si wafers with a thickness of 0.5 mm. An image plate positioned behind the sample was used to record the images with an exposure time of $\sim$10 s each. The incident beam was polarized in the horizontal direction. Data were taken with the sample in air, in a helium atmosphere, or in vacuum with similar results. The data shown below were taken with the sample in air.

Figures 1(a) and 1(b) are experimental pictures of Si(111) and Si(100), respectively. Figures 1(c) and 1(d) are the corresponding model calculations to be discussed below. The differences between experiment and calculation are too small to be visible to the eye, except for the shadows of a circular beam stop at the center of each experimental picture and a supporting post. At the center of the shadow of the beam stop is a tiny bright spot caused by the direct beam passing through the 2-mm molybdenum in the beam stop. It is a measure of the beam size and the picture resolution. By virtue of the wavelength selected, the Bragg condition is never satisfied over the entire area of detection. Thus, none of the bright spots are caused by crystal diffraction. One can readily see the symmetry of the pattern. The picture is threefold symmetric for the (111) sample, and fourfold for the (100) sample.

Each point in the picture corresponds to a planar projection of a unique momentum transfer $\mathbf{q}$ on the Ewald sphere. Because each unit cell of Si contains two atoms, there can

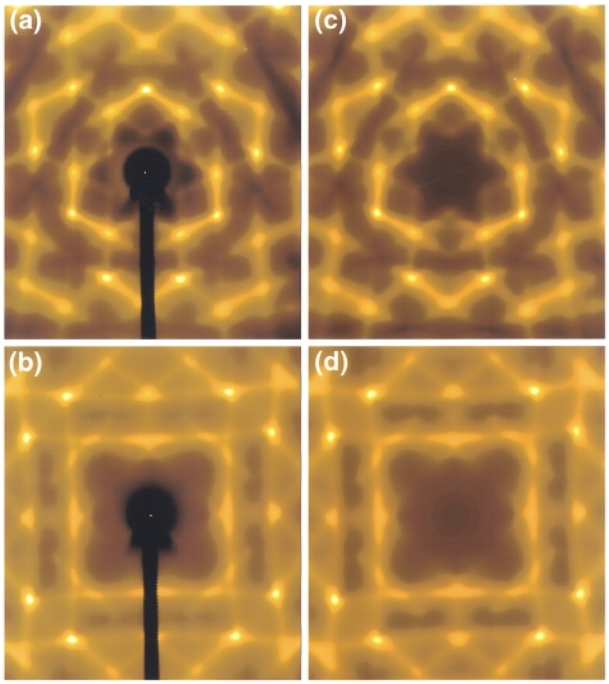

FIG. 1 (color). Transmission x-ray scattering images taken from (a) Si(111) and (b) Si(100), respectively. In each case, the shadows of a beam stop and its post are evident. The corresponding calculated images based on a best simultaneous pixel-by-pixel fit to the two experimental images are shown in (c) and (d).

be up to six distinct phonon modes (three optical modes and three acoustic) at each $\mathbf{q}$ contributing to the scattering intensity. The bright spots in each picture are points on the Ewald sphere that are closest to neighboring reciprocal lattice points, where the thermal acoustic phonon population is high. The center of the picture is dark despite the high acoustic phonon population because of a q^2 dependence in the cross section. The diffuse lines connecting the bright spots are associated with high symmetry directions where the phonon is soft and has a high density of states. The rich structure of the picture is a direct consequence of the use of a logarithmic intensity scale. This is analogous to the use of a logarithmic scale for x-ray truncation rod analysis, making it possible to detect the contribution from one surface atomic layer within a spectrum dominated by bulk contributions [9]. In the present case, the logarithmic function largely compensates for the thermal population factor, and thus, the phonon modes at different energies contribute to the intensity in an approximately linear manner. Without this logarithmic conversion, the acoustic phonon contribution near reciprocal lattice points would be the only features seen.

The theoretical pictures and phonon dispersions are derived from a force-constant formalism of the lattice dynamics, also known as the Born–von Karman model [10–12]. Force constants up to the sixth nearest neighbors are included in a harmonic lattice model, and diagonolizing the dynamic matrix results in the phonon eigenmodes. The intensity of scattering by an unpolarized incident x ray at a given momentum transfer $\mathbf{q}$ is given by a sum over the contributions from the six phonon branches [7],

$$I_0 \propto f^2 e^{-2M} \sum_{j=1}^{6} \frac{|\mathbf{q} \cdot \hat{\mathbf{e}}_j|^2}{\omega_j} \coth\left(\frac{\hbar\omega_j}{2k_B T}\right). \quad (1)$$

In this equation, f is the atomic scattering factor, M is the Debye-Waller factor [13], ω is the phonon frequency, $\hat{\mathbf{e}}$ is the polarization vector of the phonon mode, k_B is the Boltzmann constant, T is the sample temperature (300 K), and j is the index for the six phonon branches. The hyperbolic cotangent function in this equation represents a sum of the Bose-Einstein distribution function and the zero-point mode occupancy.

The calculated intensity in each pixel, on a logarithmic scale, is given by

$$I_{\text{theory}} = D \log\{[\sin^2\phi + \cos^2\phi \cos^2(2\theta)] \times (AI_0 + B)\cos(2\theta) + C\}. \quad (2)$$

In this equation, ϕ is the azimuthal angle between the plane of polarization of the incident beam and the scattering plane, and 2θ is the scattering angle. The expression within the brackets containing these angles accounts for the linear polarization of the incident beam. The quantity A is an intensity factor, B represents a background from higher order and defect scattering from the sample, C represents a uniform background, and D is an overall scaling factor related to the image plate response function. The additional factor of $\cos(2\theta)$ in the formula is for solid angle conversion associated with planar projection on the flat image plate.

Equations (1) and (2) are used to generate theoretical patterns, which are compared to the experimental ones. The shadows of the beam stop and post are excluded from this comparison by using a mask function. A least-squares algorithm is employed for a simultaneous pixel-by-pixel fit to both experimental pictures shown in Fig. 1. The fitting parameters include the force constants, the scaling and background parameters A, B, C, and D in Eq. (2), three Euler angles specifying the exact crystallographic orientation of the sample in each case, and the exact distance from the sample to the detector. The best fits are shown in Fig. 1, and the corresponding phonon dispersion curves are shown as solid curves in Fig. 2. The stability and uniqueness of the fit were established by randomly generating new starting points within a 10% Gaussian error of the starting adjustable parameters, and the final parameters returned to the same best set. The agreement with available neutron data, presented in Fig. 2 as circles, is excellent, thus validating the present method as a technique for determination of phonon dispersions. The dotted curves in Fig. 2 are obtained from an independent fit to the neutron data points using the same lattice dynamics model, and can be regarded as a k-space interpolation of the neutron data. The two sets of curves, solid and dotted, are

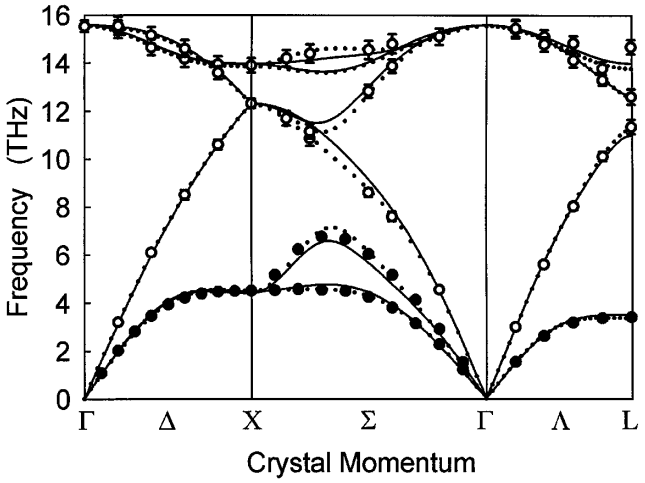

FIG. 2. Phonon dispersion curves of Si. Open circles are neutron scattering data from Ref. [3] (error bars shown), and closed circles are neutron data from Ref. [4] (error on the order of the size of the circle). Solid curves are derived from a best fit to the x-ray scattering intensity patterns shown in Fig. 1. Dotted curves are obtained from an independent fit to the neutron data using the same lattice dynamics model and can be regarded as an interpolation of the neutron data.

very close. The small differences, mostly no larger than the error bars associated with the neutron data, suggest that the accuracy of the present approach is similar to that of neutron scattering.

Many areas of experimental condensed matter physics would benefit from an alternative to neutron scattering or inelastic x-ray scattering to establish phonon properties. The present method is simple and straightforward requiring no elaborate sample alignment or complicated detector control. There are few restrictions in the applicability of this method, and high quality images have been obtained for a variety of materials, including semiconductors, metals, ionic solids, glasses, and multielement compounds. In all of these studies, bulk impurities and surface contaminants have not posed a problem. The only exception is the case of a heavily oxidized aluminum single crystal; the surface oxide layer gives rise to a faint pattern of rings superimposed on the phonon pattern. Some of these experiments involve the use of ultrahigh vacuum chambers and cryostats, and scattering from chamber walls and windows has not been a problem. The data collection rate can be as fast as 10 ms per image with an optimized setup using a charge-coupled device area detector, which is fast enough for dynamic studies (such as phase transitions). The total scattering volume required is very small, and future development of microbeams at the Advanced Photon Source will allow phonon studies of single grains in materials of practical interest. Another area of interest is the study of high pressure effects, which has been difficult with neutrons.

In summary, this work establishes x-ray phonon scattering patterns as a powerful technique for measuring phonon properties. Entire sets of dispersion curves can be derived based on data taken in seconds. This is demonstrated using Si as a test case; a simultaneous fit of the (100) and (111) patterns yields phonon dispersion curves as accurate as neutron scattering results.

This work is supported by the U.S. Department of Energy (Division of Materials Sciences, Office of Basic Energy Sciences) under Grant No. DEFG02-91ER45439. The UNICAT facility at the Advanced Photon Source (APS) is supported by the University of Illinois Frederick Seitz Materials Research Laboratory (U.S. Department of Energy, the State of Illinois-IBHE-HECA, and the National Science Foundation), the Oak Ridge National Laboratory (U.S. Department of Energy under contract with Lockheed Martin Energy Research), the National Institute of Standards and Technology (U.S. Department of Commerce), and UOP LLC. The APS is supported by the U.S. Department of Energy, Office of Science, under Contract No. W-31-109-ENG-38. Acknowledgments are also made to the Donors of the Petroleum Research Fund, administered by the American Chemical Society, and to the National Science Foundation Grants No. DMR-99-75182 and No. 99-75470 (T. C. C.) for partial equipment support in connection with the synchrotron beam line operation. The authors wish to thank DNDCAT and BIOCAT for the use of their image plate readers. They have also benefited from discussions with Z. Zhong and J. Hastings of the Brookhaven National Laboratory, who have performed similar measurements.

*To whom correspondence should be addressed.
Email address: t-chiang@uiuc.edu

[1] N. W. Ashcroft and N. D. Mermin, *Solid State Physics* (Saunders College, Philadelphia, 1976).
[2] *Dynamics of Solids and Liquids by Neutron Scattering*, edited by S. W. Lovesey and T. Springer (Springer-Verlag, New York, 1977).
[3] G. Dolling, *Inelastic Scattering of Neutrons in Solids and Liquids* (IAEA, Vienna, 1963).
[4] G. Nilsson and G. Nelin, Phys. Rev. B **6**, 3777 (1972).
[5] M. Schwoerer-Bohning, A. T. Macrander, and D. A. Arms, Phys. Rev. Lett. **80**, 5572 (1998).
[6] K. Lonsdale, *Crystals and X-Rays* (G. Bell, London, 1948).
[7] B. E. Warren, *X-Ray Diffraction* (Dover, New York, 1969).
[8] Z. Wu *et al.*, Phys. Rev. B **59**, 3283 (1999).
[9] I. K. Robinson and D. J. Tweet, Rep. Prog. Phys. **55**, 599 (1992).
[10] F. Herman, J. Phys. Chem. Solids **8**, 405 (1959). An error in this work was pointed out by C. Patel, W. F. Sherman, and G. R. Wilkinson, J. Phys. C **17**, 6063 (1984).
[11] J. P. Wolfe, *Imaging Phonons* (Cambridge University, Cambridge, England, 1998).
[12] S. Wei and M. Y. Chou, Phys. Rev. B **50**, 221 (1994).
[13] M. Deutsch and M. Hart, Phys. Rev. B **31**, 3846 (1985).